Sensitivity Analysis of Online Oil Quality Monitoring for Early Detection of Water Ingress in Marine Propulsion Systems

Andreas Klausen[1], Johannes Kalaoja[2], Surya Teja Kandukuri[3], and Kjell G. Robbersmyr [4]

[1,2,3,4] *Dept. of Engineering Sciences, University of Agder, Jon Lilletuns vei 9, Grimstad, Norway 4879*
andreas.klausen@uia.no, surya.kandukuri@uia.no, kjell.g.robbersmyr@uia.no

Abstract

Gearboxes are critical equipment in the vessel propulsion system. Lubrication contamination caused by water ingress or condensation is one of the major failure modes in marine gearboxes leading to accelerated aging of lubricant, resulting in accelerated wear of gearbox components such as bearing and gears. This article presents a systematic evaluation of moisture ingress sensitivity of three commercial online oil quality monitoring sensors. A laboratory setup consisting of an industrial multi-stage planetary gearbox is utilised for the experimental studies. Furthermore, the gearbox vibration signatures are analysed to investigate the sensitivity of vibration measurements to water ingress to determine the need for oil quality monitoring when considering this specific failure mode.

1. Introduction

Gearboxes are critical components in marine propulsion systems. Gearbox failures can result in significant breakdown and towage costs that can potentially lead to millions of US dollars in loss (The Swedish Club, 2018). In many cases, repair of propulsion gearboxes in ships requires dry-docking and hull teardown to access the equipment, and thus the repairs are time-taking, resulting in longer downtimes. Therefore, condition monitoring of gearboxes is an important aspect to ensure reliable and economical vessel operations.

Gearboxes can fail in several ways; for instance, faulty bearings (Feng, Ma, & Zuo, 2016) and wear on gear teeth (Cao, Zhang, Wang, Wang, & Peng, 2019) can result in breakdown. These faults can be detected by means of non-invasive techniques using vibration monitoring (Singh & Parey, 2019), motor current measurement (Feng, Chen, & Zuo, 2019) or acoustic emission (Elasha, Greaves, Mba, & Fang, 2017). However, the oil itself can be analysed to detect early stage faults in the gearbox as the material dislodged due to wear accumulates in the lubricant. In fact, oil debris monitoring (ODM) can detect wear and chipping of gears with an accuracy comparable to that of vibration signatures, with an advantage of being insensitive to load variations (Dempsey, 2000). Typically, the vessels conduct an accurate oil quality assessment offline at a laboratory by sending a sample (Sheng, 2016; Liu, Liu, Xie, & Yao, 2000). However, this is largely inadequate for early fault detection and failure prevention as the faults can progress significantly before the results are obtained.

Today, there are several commercial sensors that can be installed either in a so-called kidney loop or in the oil sump, to detect these ferrous or non-ferrous debris as well as other particulate and fluid contaminants in oil (Zhu, Zhong, & Zhe, 2017). Online oil quality assessment for rotating machinery has received considerable attention in research as well as in the industry. Sheng (Sheng, 2016) analysed the efficiency of using online monitoring of ferrous and non-ferrous debris in wind turbine gearboxes. Myshkin et al. (Myshkin & Markova, 2018) studied optical debris monitoring in industrial applications for detection of ferrous debris. Dempsey et al. (Dempsey & Afjeh, 2002) developed an integrated monitoring system using wear debris measurement and vibration analysis for gear health monitoring using fuzzy logic classifier. However, moisture detection is relatively less addressed and hence the central topic of this article.

Water in oil is one of the most destructive contaminants to lubrication (Lancaster, 1990). Water can enter the oil from a variety of sources such as a humid environment (Cen, Morina, Neville, Pasaribu, & Nedelcu, 2012), absorption and condensation (Cen et al., 2012). Water ingress (Soltanahmadi, Morina, van Eijk, Nedelcu, & Neville, 2017; Hamilton & Quail, 2011) cause the efficiency of the oil to diminish, reduce film production and lead to corrosion (Hamilton & Quail, 2011). With diminished oil quality, wear on bearing and gear surfaces accelerate significantly (Schatzberg, 1971). Hence, it is important to detect water in the oil to avoid accelerated failure.

In this paper, three different commercially available sensors

Table 1. Electromagnetic properties of oil and water (Lenntech, 2020; Archer & Wang, 1990; Engineering Toolbox, 2016; Bock, 2014).

Materials	Electrical conductivity	Relative permeability	Dielectric constant
Mineral oil	$6 \cdot 10^{-12}\, S/m$	~ 1	$2.1 - 2.4$
Water	$0.0005 - 0.05\, S/m$	0.999902	$87.9(0°C) - 55.5(100°C)$

are tested for their ability to detect water in the oil besides other contaminants. These sensors operate based on different measurement methods: magnetic, electrical impedance and inductive sensing. The aim is to determine the solution of the three tested sensors that has highest sensitivity for water ingress. In addition, the effect of water ingress on the vibration signature is also studied. Changes in vibration signature in a fixed-axis gearbox was reported in (Brethee, Gu, & Ball, 2017), but the results indicate low sensitivity to diagnose water ingress. Here, the vibration changes will be analysed on a planetary gearbox rather than a fixed-axis one. The objective of this analysis is to determine a minimal sensor suite to detect failures in gearboxes in addition to lubrication contamination.

The rest of the paper is organized as follows. The effect of water in oil is briefly discussed in Section 2. Section 3 introduces the test setup and the sensors involved for measuring the water ingress. The following Section 4 explains the methodology used for performing the tests. Results and discussions are given in Section 5. Finally, conclusions are drawn in Section 6.

2. WATER IN OIL

Water in oil is considered to be one of the most destructive contaminants resulting in failure of film formation between metallic contacts. A high amount of moisture content in oils can result in oxidation of oil, hydrogen generation, corrosion, and accelerated wear of metal components. In the case of bearings, it was found to be the second most destructive lubrication contaminant for bearings resulting in reduction of bearing life by more than 100 times (Fitch & Jaggernauth, 1994). While oils are hygroscopic in nature and absorb a small amount of moisture from atmosphere, the marine water ingress, either as dissolved, from condensation, free water, or leaks, can be particularly detrimental to the rotating machinery due to dissolved salts. Free water forms an emulsion which decreases lubricant load carrying capacity (Stachowiak & Batchelor, 2013). Saturation limits depend on chemical characteristics of the oil, additives, the oil condition (Needelman, Barris, LaVallee, et al., 2009), and the environment such as temperature and relative humidity (Troyer, 1998; Day & Bauer, 2007). For a detailed insight into the tribological aspects of water in oil, the interested reader can refer to (Cantley, 1977). Besides, the presence of water changes the oil film quality in gear contacts, hence making it interesting to study the impact of water ingress on the vibration signature.

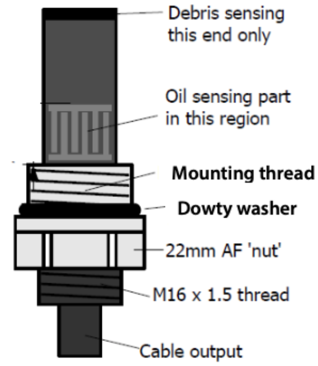

Figure 1. Commercial magnetic oil quality sensor. Courtesy: Gill SC (Limited, 2018).

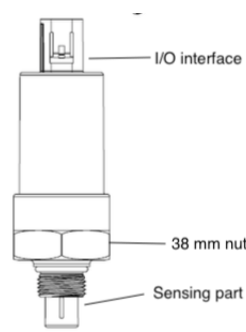

Figure 2. EIS sensor. Courtesy: Poseidon Systems (Poseidon Systems, 2018).

The presence of water changes the electrochemical properties of the lubricant. The electric characteristics of the lubricant and water are shown in Table 1. Due to the large discrepancies in electrical characteristics between mineral oil and water, the water ingress may be distinguishable using sensors that can measure the dielectric constant or other electrical properties. In this article, three types of oil quality sensors shall be evaluated, shown in Table 2. The objective behind the evaluation is to ensure the acceptable observability of water ingress in lubrication with reasonable cost vs. benefit to facilitate economical fleet-level deployment of gearbox health monitoring in vessels.

- *Magnetic sensor*

Table 2. Oil quality sensors in testing.

#	Manufacturer	Part no.	Product description
1	Gill	4212-00-038	Magnetic oil condition sensor
2	Poseidon	Trident QW3100 PS-0113-0200	Electrical impedance sensor for oil contamination
3	Parker	Kittiwake AS-K19551-KW	Inductive coil sensor for metallic wear debris detection

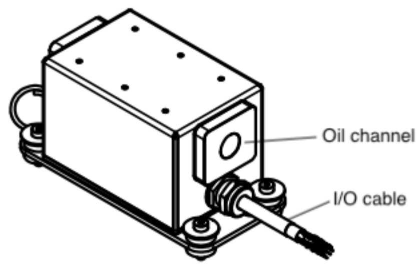

Figure 3. Metallic wear debris sensor. Courtesy: Parker (Kittiwake, 2019).

Sensor #1 is a magnetic sensor that can detect and collect ferrous materials in the lubricant (Limited, 2018) as shown in Fig. 1. The sensor consists of magnetic and electromagnetic elements to attract and collect ferrous debris in oil. The sensor can differentiate between fine and course particles, where the boundary between fine and course is around 1-2 mm. In addition, the sensor also has a dielectric element which can detect change in oil quality and oil level. The sensor is capable of detecting presence of water in oil, but the claim is that the water content should be at least at 10% concentration. The magnetic sensor can either be mounted in the oil sump within the gearbox or within the kidney loop. In fact, this is the only one among the tested sensors that does not require a kidney loop, and is thus suitable for gearboxes where adding such a loop is not feasible.

- *Electrochemical impedance spectroscopy sensor*
  Sensor #2 shown in Fig. 2 uses electrochemical impedance spectroscopy (EIS) to estimate the health of the lubricant (Poseidon Systems, 2018). The EIS measurement technique applies AC voltage and measures the resulting current to determine the impedance. Performing this at different voltage frequencies allows for identifying the impedance frequency response of the lubricant.
  The impedance is dependent on the lubricant type and the amount of contaminants. Since metallic debris generally has a higher electric conductivity compared to lubricant, the impedance should decrease when the lubricant is contaminated with metallic debris. Water also inherit higher electrical conductivity than most lubricants. In addition to this sensing technology, the sensor can also detect the relative humidity in the lubricant thanks to a dielectric element. The EIS sensor is reported to be a versatile oil quality sensor capable of detecting magnetic and non-magnetic debris as well as other contaminants such as soot and humidity in engine oils (Fecek, 2017).

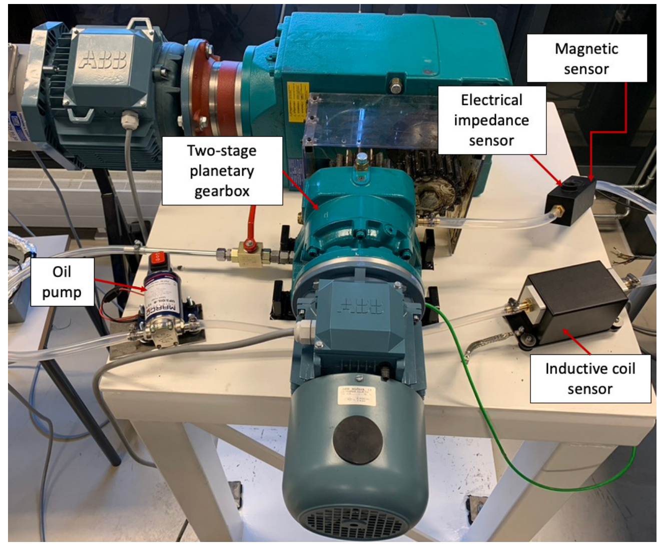

Figure 4. Test-bench consisting of two-stage planetary gearbox for seeded fault tests with three types of online oil monitoring sensors.

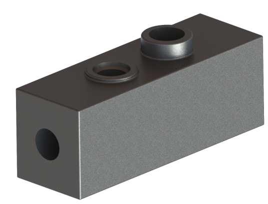

Figure 5. 3D printed sensor block for sensors 1 and 2.

- *Metallic wear debris sensor*
  Sensor #3, shown in Fig. 3, is a metallic wear debris sensor (MWDS) that is mainly relevant for detecting ferrous and non-ferrous metal in the lubricant (Kittiwake, 2019). The sensor measures the electromagnetic properties of the lubricant using an inductive coil technology. This also results in reading of the electrical conductivity and magnetic permeability of metal particles in the lubricant. The sensor can report the particle count, the number of particles per minute (ppm), and also whether the particles are ferrous or non-ferrous. This sensor does not have a dedicated measurement for water ingress, and the results may not be relevant for this particular study.

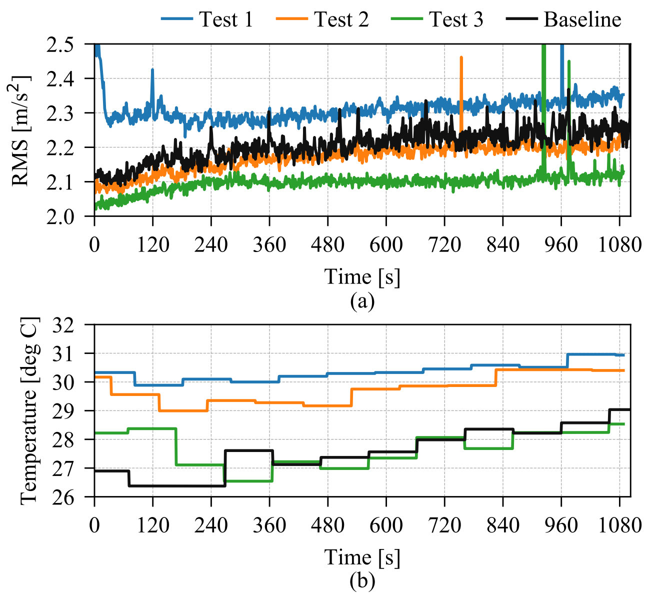

Figure 6. Three tests with water ingress. 0.25 mL of water is added every 120 seconds, up to a total of 2 mL. (a) Vibration RMS; (b) Oil temperature measured using sensor 2 (Poseidon Trident).

3. EXPERIMENTAL TEST SETUP

A laboratory test setup shown in Fig. 4 was built to evaluate several failure modes in electromechanical drives. The test setup consists of a 'two-stage planetary gearbox' with a gear ratio $i = 48.1$, driven by a 1.1 kW three-phase induction motor. The gearbox is coupled to a bevel-planetary-helical 'load gearbox' with a gear ratio of $i = 27$ through a $1 : 1$ open spur-gear coupling. The load gearbox is driven by 3 kW three-phase induction motor. Both the motors are inverter-fed and controlled in closed-loop using commercial controllers. An oil circulating loop, the so-called kidney loop, is connected to the planetary gearbox to recirculate the lubricant in the gearbox using a DC oil pump. The three oil quality sensors are placed in the loop for online oil quality measurements. Sensors 1 and 2 are mounted on a 3D printed sensor block shown in Fig. 5, while sensor 3 is connected directly in the loop. Besides, an accelerometer with a range of ± 20 g's and sensitivity of ≈ 100 mV/g is installed on the gearbox to measure radial accelerations for vibration analysis. The testing procedure is described in the following section.

4. TESTING METHODOLOGY

Initially, the gearbox was flushed, and fresh oil was added. Water is added in small portions using a syringe to check the sensor sensitivity at small increments of water ingress. The amount of water is calculated based on a required ppm value. The tests are conducted when the oil and gearbox are at room temperature. The experiment was repeated three times with

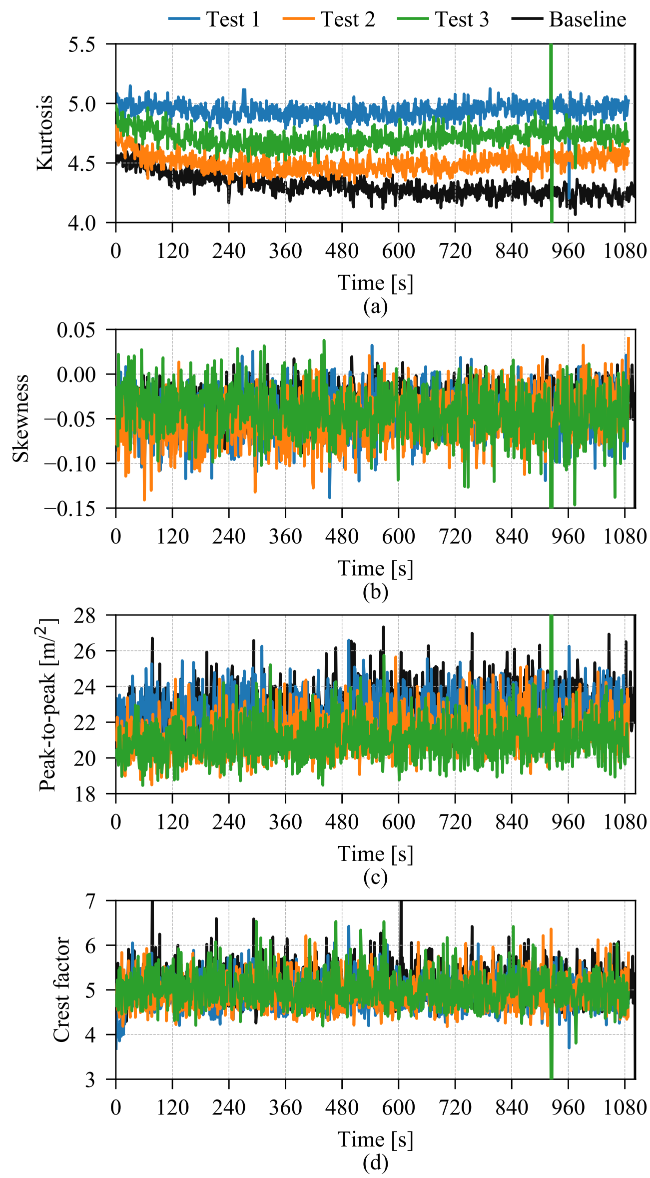

Figure 7. Three tests with water ingress. 0.25 mL of water is added every 120 seconds, up to a total of 2 mL. Other vibration features are checked (a) Kurtosis; (b) Skewness; (c) Peak-to-peak; (d) Crest factor.

fresh oil to assess the repeatability of the results. The gearbox combined with the recirculation loop holds 1.5 L of VG 150 gear oil. This amount is the basis for performing the experiments, as the oil saturation levels are based on ppm values. To ensure that enough water is added to saturate the oil, up to 1300 ppm of water is added, which is 2 mL.

During testing, the total amount of water is added in 8 steps of 0.25 mL. In this way, the sensors can be checked for their ability to detect water ingress early. The water used is regular (potable) tap water. The oil circulation pump moves 5.5 L/min, which makes the circulation time of 1.5 L to be

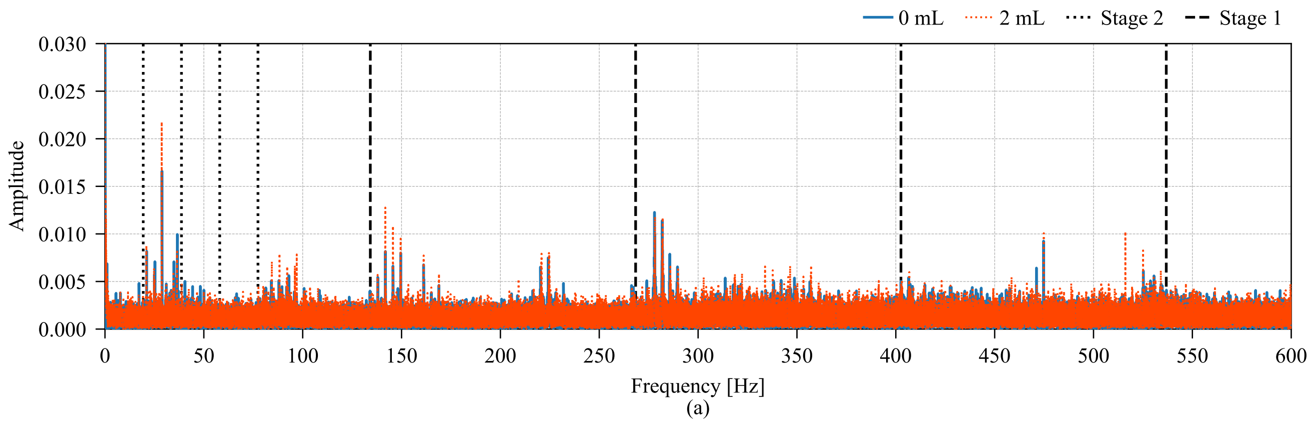

Figure 8. Comparing FFT of vibration signal between baseline and adding 2 mL of water. The first four harmonics of the mesh frequency of both stages are shown as the stapled lines.

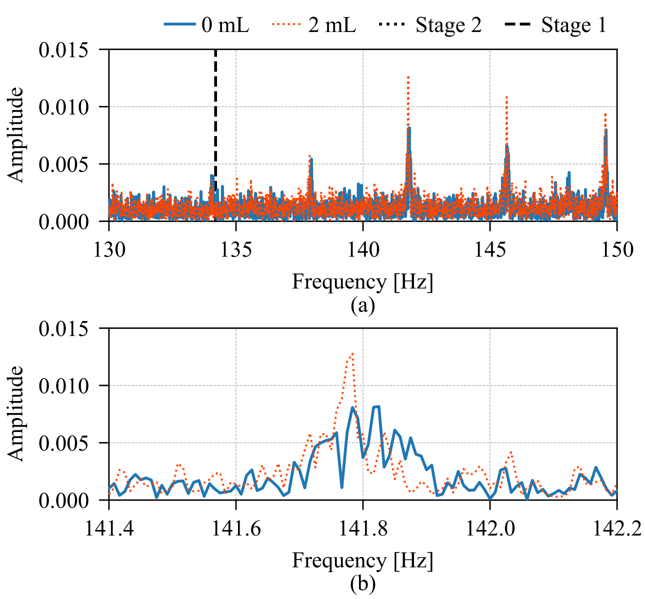

Figure 9. Comparing FFT near mesh frequency of vibration signal between baseline and adding 2 mL of water. (a) Centered around 1st mesh harmonic; (b) Zoomed in of highest red-stapled peak in subfig (a).

roughly 16 seconds. Within a time frame of 120 seconds, the oil should have been circulated 7.5 times, which should be enough for the water to properly mix in the oil. Therefore, more water is added in steps every 120 seconds. The induction motor is run at a near-constant speed of 600 rpm, where small speed fluctuations may occur due to inadequate controller performance at low speeds.

5. RESULTS AND DISCUSSIONS

As mentioned in the testing methodology, three tests of water ingress are performed to assess the repeatability. These three tests will be referred to as "Test 1" through "Test 3" in this section. In addition, there is a "Baseline" reference where no water is added over the same test duration. For each test, the motor vibration and oil condition sensors are measured for the duration of adding the 2 mL in steps. That is a total of 120 seconds + 8 times 120 seconds, totalling 1080 seconds.

The vibration signal is first analysed to determine whether it is suitable for early water ingress detection. The vibration signal is split into segments of 1.2 seconds, and the root mean square (RMS) is calculated for each segment using the following:

$$\text{RMS}(x) = \sqrt{\frac{1}{N}\sum_{i=1}^{N} x_i^2}\,, \tag{1}$$

where x is the vibration segment and N is the number of samples in the segment. Figs. 6 (a) and (b) show the vibration RMS from accelerometer, and oil temperature measured using sensor 2, respectively. As seen, the RMS values are ranging between 2 and 2.4 m/s^2 and appears to be slightly dependent on the current oil temperature. On tests 1-3, the RMS value increases slightly from start till finish, which could indicate a change in condition. However, as the baseline RMS also increases over time, we cannot conclude that the RMS increase occurs due to water ingress. The increase may be due to the temperature increase, which reduces the viscosity, hence reducing oil film thickness increasing the vibration energy.

To further validate that the vibration signal is not largely dependent on water ingress, several other vibration features are calculated and shown in Fig. 7.

Here, the kurtosis (measure of impulsivity), skewness (measure of asymmetry), peak-to-peak and crest factor (measure of extreme peaks) are calculated over the duration of the tests

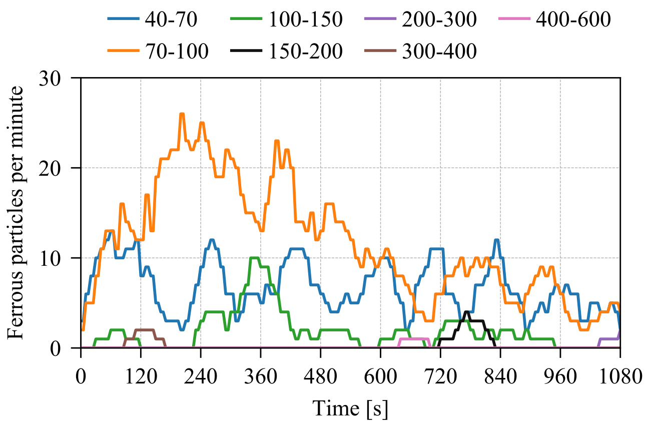

Figure 10. Ferrous particle flow measured with sensor 3 during test 1. The legend entries indicate size ranges in µm.

using the following equations:

$$\text{Kurtosis}(x) = \mu_4/\sigma^4 \quad (2)$$
$$\text{Skewness}(x) = \mu_3/\sigma^3 \quad (3)$$
$$\text{Peak-to-peak}(x) = \max(x) - \min(x) \quad (4)$$
$$\text{Crest factor}(x) = \max(x)/\text{RMS}(x)\,. \quad (5)$$

where μ_4 and μ_3 are the fourth and third central moment of x, respectively and σ is the standard deviation of x. As shown in the figure, are no significant changes in these features from adding water to the gearbox. Only the kurtosis value in 7 (a) is changing slightly over time, but so does the baseline measurement. Therefore, we cannot conclude that these features will aid in detecting early water ingress.

To further investigate any changes in vibration signature, the frequency spectrum is acquired using the fast Fourier transform (FFT). To limit the differences in temperature, one vibration segment of 120 second is taken between 960 seconds and 1080 seconds of the baseline, and the same time window of test 3, since the temperature is similar in Fig. 6 (a). In this time window, 0 mL and 2 mL water ingress is compared. The two spectra are shown in Fig. 8, where the blue line is baseline at 0 mL, and red stapled is after adding 2 mL water.

The most interesting part is the increased energy at the mesh frequency, as decreased oil performance could increase meshing vibration energy. In Fig. 8 the harmonics of meshing frequency of the two stages inside the planetary gearboxes are shown as stapled lines, as indicated by the legend. There is no apparent energy increase at the harmonics of the mesh frequency itself, but there are some other peaks that appear to have increased in value, especially near the first harmonic of meshing at stage 1. This area is shown more clearly in Fig. 9 (a).

The four peaks seen to the right of the meshing frequency in Fig. 9 (a) are possibly not related directly to the plane-

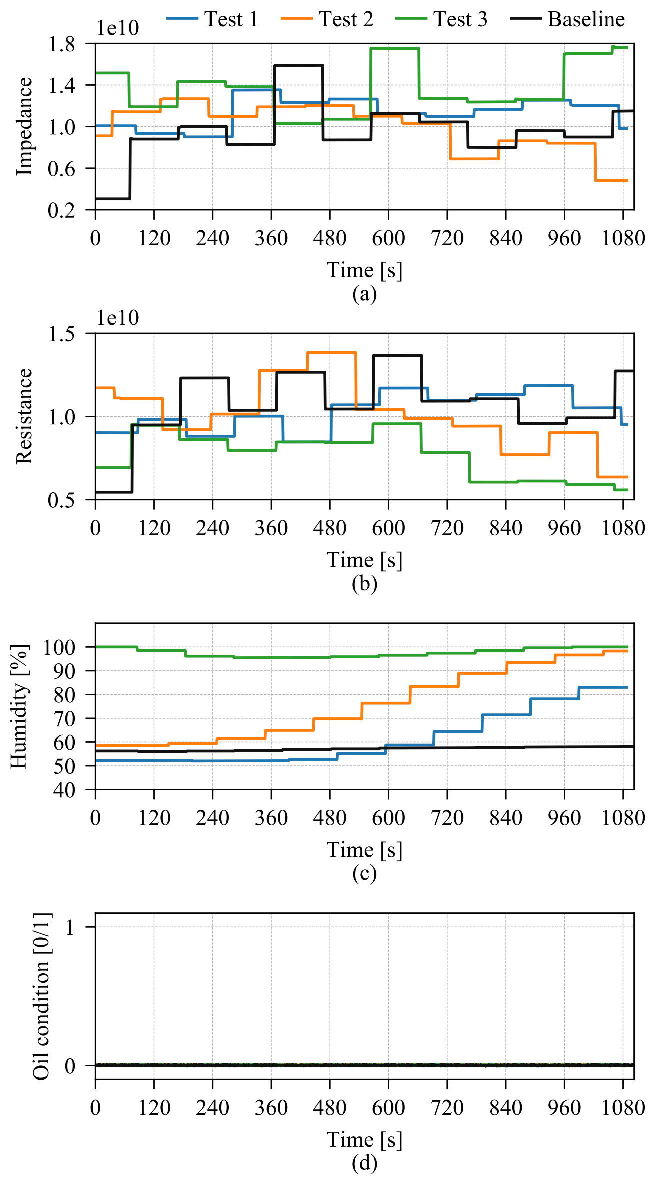

Figure 11. Three tests with water ingress. 0.25 mL of water is added every 120 seconds, up to a total of 2 mL. (a) Oil impedance; (b) Oil resistance; (c) Oil humidity; (d) Oil condition trigger.

tary gearbox but due to the spur gear coupling between the planetary gearbox and the load gearbox shown in Fig. 4, and the sub-band spacing between the four peaks matches the meshing frequency of this spur gear. As this lab setup is newly setup, this spur gear may not have been properly aligned, hence creating high vibration energy at this meshing frequency. The notable peaks in 9 (a) may, therefore, be amplitude modulations of the meshing vibration of stage 1 inside the planetary gearbox. Even if this is the case, the energies at these peaks can still be compared further. The highest valued peak near 141.8 Hz is shown further in Fig. 9 (b). While the

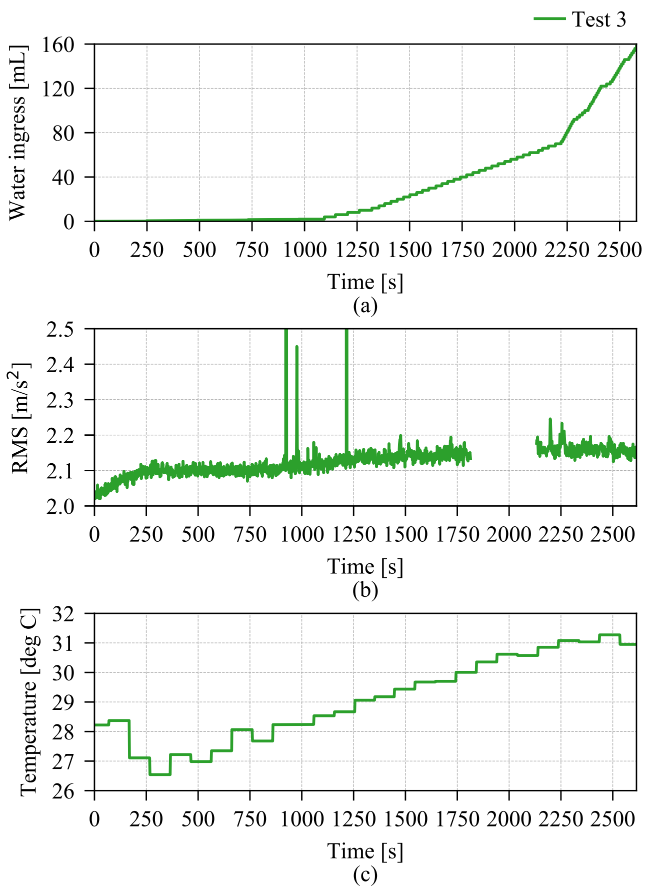

Figure 12. Continuation of test 3 test after adding 2 mL of water. (a) Vibration RMS; (b) Oil temperature at sensor 2; (c) Water ingress content.

red-stapled line has a higher maximum value, it appears to be less spread than the blue baseline plot. Hence, the energy content may actually be the same around this frequency, just more spread on the baseline measurements, which makes it hard to determine any real changes between the baseline and 2 mL water ingress test.

The data from the commercial oil quality sensors are also analysed to determine which is best suited for early detection of water ingress. First, we investigate the least probable one for water ingress, namely sensor 3 the Parker Kittiwake. This sensor is mostly used for detecting ferrous and non-ferrous metallic debris. However, it is investigated to determine if its measurements are affected by the water ingress since the oils impedance may change. Fig. 10 shows the resulting measurements from this sensor.

Measured ferrous sediments in the range 70-100 µm increases in the beginning of the test, but slowly decreases near the end. The other sizes are mostly static or periodic over the test. However, there is no clear indication that the sensor is affected by the water ingress, since none of the values are increasing over time. The sediments in range 70-100 µm may be decreasing since sensor 1 from Gill is magnetic and captures ferrous particles as they pass the sensor. The origin of these sediments is not known, but may stem from gear fatigue.

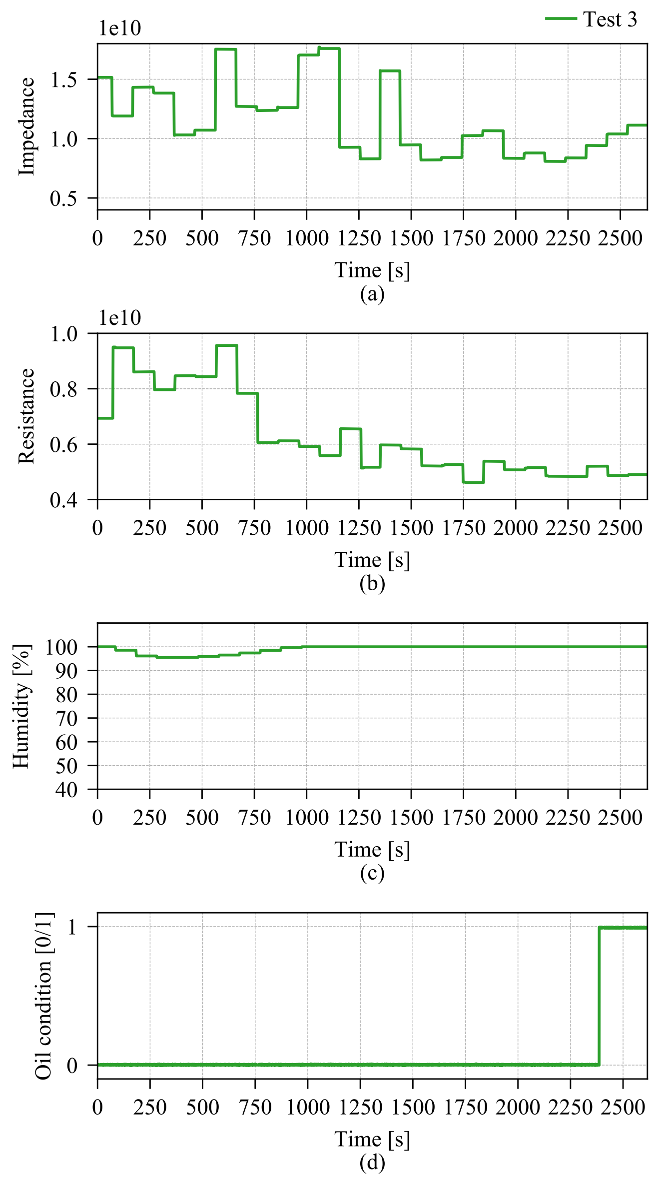

Figure 13. Continuation of test 3 test after adding 2 mL of water. (a) Oil impedance; (b) Oil resistance; (c) Oil humidity; (d) Oil condition trigger.

Finally, sensors 1 and 2 are checked for their response to the water ingress. Fig. 11 shows the available measurements relevant for water ingress. Subplots (a), (b) and (c) are the oil impedance, oil resistance and humidity percentage reported by sensor 2 Poseidon Trident, respectively. Subplot (d) is a binary trigger given by sensor 1 from Gill that should, according to the manufacturer (Limited, 2018), turn positive if

Table 3. Comparison of the three commercial sensors with respect to water ingress detection

Property	**Sensor 1**	**Sensor 2**	**Sensor 3**
Cost	X	3X	10X
Sensitivity to water	Can detect large water ingress (>10% of the oil)	Highly sensitive to water ingress. Can detect changes before reaching 1000 ppm	Does not indicate any changes to water ingress
Installation mode	Flexible; Can be installed either in oil sump or in a kidney loop	Can be installed only in a kidney loop. Additional housing or drilling necessary	Can be installed in a kidney loop, no additional housing required
Advantages	Low cost; Can collect ferrous debris to avoid pump damage	EIS is capable of detecting multiple contaminants. Qualitative indication of contaminants in terms of resistance and impedance	Highly specialized. Quantitative measurements of debris sizes indicating type of material and severity of fatigue
Disadvantages	Accuracy of the measurement depends on the ability to attract magnetic particles, therefore, sensitive to sensor location	Skilled personnel necessary to interpret the results	Expensive and specialized

water content exceeds 10 % (100 000 ppm). As seen in Figs. 11 (a) and (b), there is no clear trend of the impedance or resistance plots that would indicate a large change in oil condition. However, while this sensor is sampled at a rate of 10 Hz, the steps in measurement values indicate that there is some internal filtering in the sensor, and it is possible that using a longer settling time than 120 seconds may reveal that these values would change in a more affirmative way.

Fig. 11 (c) shows the humidity percentage which changes almost proportionally with the addition of water ingress. Here, the values are clearly changing compared to the baseline. Initially, on test 1 and 2, the humidity rises from roughly 50% to 80-100%, while the baseline measurements show a constant humidity. However, it is apparent that the gearbox was not properly flushed between test 2 and 3, since the humidity starts at 100%. In any case, tests 1 and 2 show that this type of measurement is superior to the previously shown results for detecting early water ingress.

The last measurement is the oil condition trigger of sensor 1, which is shown in Fig. 11 (d). As expected, this trigger does not activate since the water content is too low, which makes this sensor unsuitable for early water ingress detection.

To force larger changes in sensor measurements, a lot more water is added after the end of test 3. The aim was to trigger the oil condition measurement of sensor 1 from Gill. To this end, up to 160 mL of water was added to the gearbox, which results in roughly 10% water content in the oil. Fig. 12 (a) shows the water ingress, where a lot more water is added rapidly after the last 0.25 mL step at 1080 seconds. In addition to this, Fig. 12 (b) shows the vibration RMS, and Fig. 12 (c) shows the oil temperature. The RMS value increases a little bit after adding significantly more water, but not by a lot, which makes it still not clearly indicative of water ingress. The temperature also increases slightly over time, which is to be expected since the test lasts longer. In hindsight, the RMS values would be easier to analyse if the oil temperature was brought to a steady state before adding water.

Finally, responses of sensors 1 and 2 are tested in this extended water ingress test. Fig. 13 shows the results when adding the extra water content. The impedance measurement in Fig. 13 (a) is erratic and even increases slightly near the end of the test, indicating a poor sensitivity to water ingress. On the other hand, the resistance in Fig. 13 (b) actually decreases quite significantly, which does indicate severe water ingress. This is attributed to the electrical conductivity in Table 1, as water leads current at a much lower resistance than typical mineral oil. The humidity measurements are, not surprisingly, still capped at 100% as shown in Fig. 13 (c). Near the end, after nearly 120 mL of water is added to the gearbox, the oil condition trigger on Sensor 1 turns from 0 to 1 in Fig. 13 (d). This is indicative of severe water ingress up to 10%, which is quite substantial. Ideally, water ingress should be detected long before reaching this high concentration.

Overall, theses tests show that the humidity measurement from sensor 2 is the most sensitive to water ingress, and the second most sensitive is its resistance measurement. Further, the vibration signature did not show a clear change due to water ingress. A more detailed comparison of the sensors with respect to their utility for water ingress detection is detailed in Table 3.

6. CONCLUSIONS

Water ingress in marine gearboxes can lead to rapid degradation in these critical components. In this article three commercial oil quality monitors are tested for their sensitivity to water ingress detection. Besides, the effect of water ingress on vibration measurements is also investigated. This is primarily to justify the additional expense of oil quality monitoring sensor on these systems in addition to vibration measurements, which are becoming commonplace. The investigation has shown that vibration monitoring alone may not be able to detect water ingress. Among the online oil quality monitoring sensors, the electrical impedance spectroscopy sensor appears to be the most sensitive to water ingress. In particular the humidity reading has the highest sensitivity of the acquired measurements. Given the criticality of this failure mode based on the vessel history, a cost vs benefit analysis may be conducted prior to large scale deployment of these sensors. In the future, the authors aim to test these sensors on ferrous and non-ferrous debris to further evaluate the benefits of incorporating these sensors in a condition monitoring system for marine gearboxes.

ACKNOWLEDGMENT

This work has been funded by the Ministry of Education and Research in Norway.

REFERENCES

Archer, D. G., & Wang, P. (1990, mar). The dielectric constant of water and debye-hückel limiting law slopes. *Journal of Physical and Chemical Reference Data*, *19*(2), 371–411. doi: 10.1063/1.555853

Bock, W. (2014). Industrial gear oils. In *Encyclopedia of lubricants and lubrication* (pp. 977–994). Springer Berlin Heidelberg. doi: 10.1007/978-3-642-22647-2_282

Brethee, K. F., Gu, F., & Ball, A. D. (2017). Monitoring of water contamination in gearbox lubricant based on vibration analysis. *COMADEM*.

Cantley, R. (1977). The effect of water in lubricating oil on bearing fatigue life. *A.S.L.E. Transactions*.

Cao, W., Zhang, H., Wang, N., Wang, H. W., & Peng, Z. X. (2019, apr). The gearbox wears state monitoring and evaluation based on on-line wear debris features. *Wear*, *426-427*, 1719–1728. doi: 10.1016/j.wear.2018.12.068

Cen, H., Morina, A., Neville, A., Pasaribu, R., & Nedelcu, I. (2012, dec). Effect of water on ZDDP anti-wear performance and related tribochemistry in lubricated steel/steel pu re sliding contacts. *Tribology International*, *56*, 47–57. doi: 10.1016/j.triboint.2012.06.011

Day, M., & Bauer, C. (2007). Water contamination in hydraulic and lube systems. *Practicing Oil Analysis*, *9*, 2007.

Dempsey, P. (2000). A comparison of vibration and oil debris gear damage detection methods applied to pitting damage. In *Nasa/tm-2000-210371*.

Dempsey, P., & Afjeh, A. A. (2002). Integrating oil debris and vibration gear damage detection technologies using fuzzy logic. *International 58th Annual Forum and Technology Display, American Helicopter Society, Montreal, Quebec, Canada (NASA/TM-2002-211126)*.

Elasha, F., Greaves, M., Mba, D., & Fang, D. (2017, jan). A comparative study of the effectiveness of vibration and acoustic emission in diagnosing a defective bearing in a planetry gearbox. *Applied Acoustics*, *115*, 181–195. doi: 10.1016/j.apacoust.2016.07.026

Engineering Toolbox. (2016). Permeability. *Available at www.engineeringtoolbox.com*.

Fecek, D. P. (2017). Online Detection of Water and Coolant in Engine Oil. *MSc Thesis, Graduate School, Pennsylvania State University*.

Feng, Z., Chen, X., & Zuo, M. J. (2019, apr). Induction motor stator current AM-FM model and demodulation analysis for planetary gearbox fault diagnosis. *IEEE Transactions on Industrial Informatics*, *15*(4), 2386–2394. doi: 10.1109/tii.2018.2875447

Feng, Z., Ma, H., & Zuo, M. J. (2016, may). Vibration signal models for fault diagnosis of planet bearings. *Journal of Sound and Vibration*, *370*, 372–393. doi: 10.1016/j.jsv.2016.01.041

Fitch, J., & Jaggernauth, S. (1994). Moisture–the second most destructive lubricant contaminate, and its effects on bearing life. *P/PM Technology*, *12*, 1–4.

Hamilton, A., & Quail, F. (2011, oct). Detailed state of the art review for the different online/inline oil analysis techniques in context of wind turbine gearboxes. *Journal of Tribology*, *133*(4). doi: 10.1115/1.4004903

Kittiwake, P. (2019). Metallic wear debris sensor instruction manual (12th ed.) [Computer software manual]. 3 - 6 Thorgate Road Littlehampton West Sussex BN17 7LU United Kingdom.

Lancaster, J. (1990). A review of the influence of environmental humidity and water on friction, lubrication and wear. *Tribology International*, *23*(6), 371 - 389.

Lenntech. (2020). Water conductivity. *Available at www.lenntech.com*.

Limited, G. S. . C. (2018, 04). Oil condition monitoring sensor user manual (5th ed.) [Computer software manual]. Unit 600, Ampress Park, Lymington, Hampshire, SO41 8LW, UK.

Liu, Y., Liu, Z., Xie, Y., & Yao, Z. (2000). Research on an on-line wear condition monitoring system for marine diesel engine. *Tribology International*, *33*(12), 829–835. doi: 10.1016/S0301-679X(00)00128-6

Myshkin, N. K., & Markova, L. V. (2018). Wear prediction for tribosystems based on debris analysis. In *On-line* *condition monitoring in industrial lubrication and tribology* (pp. 131–201). Springer International Publishing.

Needelman, W. M., Barris, M. A., LaVallee, G. L., et al. (2009). Contamination control for wind turbine gearboxes. *Power Engineering*, *113*(11), 112.

Poseidon Systems, L. (2018, 05). Trident qm3100™/qw3100™user's manual (C ed.) [Computer software manual]. 200 Canal View Blvd. Rochester, NY 14623.

Schatzberg, P. (1971, apr). Inhibition of water-accelerated rolling-contact fatigue. *Journal of Lubrication Technology*, *93*(2), 231–233. doi: 10.1115/1.3451546

Sheng, S. (2016, jan). Monitoring of wind turbine gearbox condition through oil and wear debris analysis: A full-scale testing perspective. *Tribology Transactions*, *59*(1), 149–162. doi: 10.1080/10402004.2015.1055621

Singh, A., & Parey, A. (2019, jan). Gearbox fault diagnosis under non-stationary conditions with independent angular re-sampling technique applied to vibration and sound emission signals. *Applied Acoustics*, *144*, 11–22. doi: 10.1016/j.apacoust.2017.04.015

Soltanahmadi, S., Morina, A., van Eijk, M. C., Nedelcu, I., & Neville, A. (2017, mar). Tribochemical study of micropitting in tribocorrosive lubricated contacts: The influence of water and relative humidity. *Tribology International*, *107*, 184–198. doi: 10.1016/j.triboint.2016.11.031

Stachowiak, G., & Batchelor, A. W. (2013). *Engineering tribology*. Butterworth-Heinemann.

The Swedish Club. (2018). Main engine damage study. *Available at* https://www.swedishclub.com.

Troyer, D. (1998). The visual crackle-a new twist to an old technique. *Practicing Oil Analysis magazine*.

Zhu, X., Zhong, C., & Zhe, J. (2017, may). Lubricating oil conditioning sensors for online machine health monitoring – A review. *Tribology International*, *109*, 473–484. doi: 10.1016/j.triboint.2017.01.015